Rocky Worlds DDT: JWST/MIRI Scheduling Report for TOI-771 b

Munazza K. Alam, Brett Morris, Tyler Baines, Rachel A. Cooper | ***RWDDT JWST Target Scheduling Team***
Néstor Espinoza, Hannah Diamond-Lowe | ***RWDDT CIT Leads***

The Rocky Worlds Director's Discretionary Time (RWDDT) program will observe 4 eclipses the rocky exoplanet TOI-771 b using MIRI Imaging photometry with the F1500W filter. As detailed below, the JWST Target Scheduling Team has refined the orbital parameters (§1) for this planet and has used these values to calculate the phase constraints and observation windows (§2), as well as the APT inputs (§3).

1 ORBITAL PARAMETER CALCULATIONS

The TOI-771 system hosts the transiting rocky planet TOI-771 b with an orbital period of 2.3 days and non-transiting outer planet TOI 771 c at period of 7.6 days (Lacedelli et al., 2025). B. Morris performed a joint fitting analysis of available public and published ground- and space-based data to generate an updated set of orbital parameters and refine the eclipse ephemerides for scheduling the upcoming RWDDT observations.

1.1 AVAILABLE DATA

We identified the following available transit and radial velocity datasets:

- space-based photometry from TESS sectors 10, 11, 12, 37, 38, 64, 65, totaling 70 transits from 2019 - 2023;
- ground-based photometry of two transits from TRAPPIST in z' and I+z' bands in 2022; and
- precise radial velocities (RVs) from ESPRESSO taken during 2023-2024.

We removed outliers from the TESS photometry that exceed 8× the median absolute deviation of the flux in each sector. We then normalized each TESS sector and TRAPPIST transit by its mean flux, and masked out TESS photometry more than four transit durations from the expected mid-transit times of TOI-771 b . We assumed that each TESS sector data product had dilution corrections applied before our analysis.

1.2 RESULTS

We adopted broad uniform priors on the system parameters, centered on the results of the joint analysis by Lacedelli et al. (2025), which were allowed to vary over a range that spans a few times the literature uncertainties. We ran two fits: one with a circular orbit, and another where the eccentricity was allowed to vary. We integrated

		TOI-771 b:	
Parameter	Prior	eccentric	circular
P [days]	$\mathcal{U}(2.3160155, 2.3360155)$	$2.3260187^{+0.0000010}_{-0.0000010}$	$2.3260184^{+0.0000009}_{-0.0000010}$
t_0 [$\mathrm{BJD_{TDB}}$ - 2458572]	$\mathcal{U}(0.4166, 0.4199)$	$0.41819^{+0.00042}_{-0.00039}$	$0.41853^{+0.00038}_{-0.00035}$
ω [deg]	$\mathcal{U}^\dagger$ or fixed	-20^{+173}_{-132}	90 (fixed)
e	$\mathcal{U}^\dagger$	$0.05^{+0.05}_{-0.03}$	0 (fixed)
b	$\mathcal{U}(0, 1)$	$0.47^{+0.08}_{-0.10}$	$0.14^{+0.12}_{-0.09}$

Table 1: Global fitting results. †For the eccentric fits, longitude of periastron ω and eccentricity e were reparameterized as $\sqrt{e}\cos\omega, \sqrt{e}\sin\omega \sim \mathcal{U}(-0.35, 0.5)$.

for posterior distributions of the system parameters from the photometry and radial velocities using `juliet` (Espinoza et al., 2019) with dynamic nested sampling from `dynesty` (Speagle, 2020) using 500 live points.

Both the circular and eccentric fits produced results consistent with Lacedelli et al. (2025). The difference in Bayesian evidence between the circular and eccentric orbits yielded $\Delta \ln \mathcal{Z} \approx 0.68$, or Bayes factor of ~ 2, insignificantly in favor of the circular orbit fit. Extrapolating the expected mid-eclipse time forward to 2026-03-08 UTC, for example, the eccentric and circular orbits agree on the mode of the eclipse time posterior PDF, while the eccentric eclipse time PDF is 78$\times$ wider than the circular eclipse time. The 1σ uncertainity on the time of eclipse is $\pm$0.02 hours for the circular case, and $\pm$1.56 hours for the eccentric case. Our fits are consistent with an offset of $\sim$1 hour between the circular and eccentric solutions.

2 OBSERVING STRATEGY

To determine the number of eclipses needed for this target, N. Espinoza and H. Diamond-Lowe followed the RWDDT 2-checkpoint strategy and calculated that 3 eclipse observations of TOI-771 b are required to reach Checkpoint 1, which is the threshold for separating a zero-albedo, no heat redistribution case from a flat line at the 3σ level with $>$80% statistical power. To reach Checkpoint 2, 4 eclipse observations of TOI-771 b are required to differentiate a CO_2-dominated atmosphere case from a zero-albedo bare rock case at 3σ with a statistical power $>$80%. In these calculations we assume JWST ETC MIRI/15 μm noise $\times 1.25$, enhanced to account for systematic and/or astrophysical noise.

T. Baines then followed the Tinker Scheduling strategy used in prior RWDDT observations (e.g., DD 9235) to calculate the observing windows and phase constraints for each of the 4 eclipses (Figure 1). The Tinker Scheduling strategy is designed to set a risk of only 10% on missing all of the eclipses (in both the eccentric and circular cases). The minimum and maximum phase, zero phase, total time on-target, and number of integrations per eclipse observation are reported in Table 2.

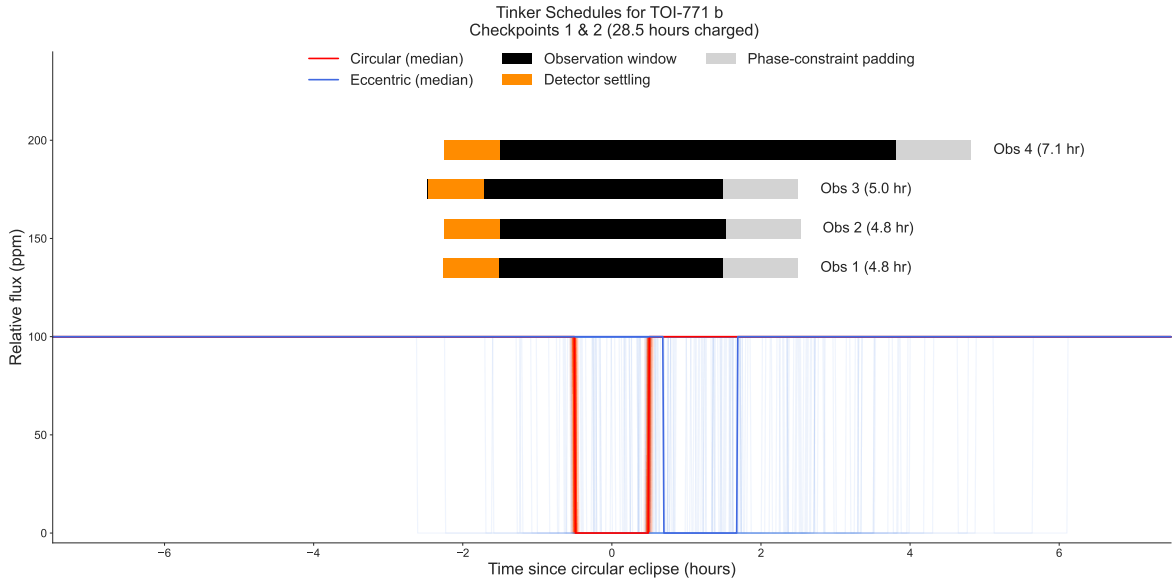

Figure 1: Observation windows for MIRI 15 μm secondary eclipses of TOI-771 b , based on the 2-checkpoint and Tinker Scheduling strategies.

3 APT INPUT CALCULATIONS

Calculations for the APT file and the ETC were performed by T. Baines and M. Alam. Using system parameters from the NASA Exoplanet Archive, we updated the mid-eclipse time, orbital period, impact parameter, and eccentricity to the best-fit values from B. Morris' circular `juliet` fits. We then calculated the optimal configuration for these MIRI Imaging time-series observations using the F1500W filter. All instrumental parameters assume a 65% saturation limit to preserve detector linearity while maximizing SNR. The selected configuration (calculated with APT 2025.1, JWST ETC 4.1, Pandeia 4.0) uses the BRIGHTSKY subarray with FASTR1 readout and 39 groups per integration (Table 3). We also retrieved the updated right ascension (RA), declination (Dec), parallax, proper motion RA, and proper motion Dec from Gaia Data Release 3 (Gaia Collaboration et al., 2016, 2023), as shown in Table 3.

M. Alam also performed ETC calculations (Workbook ID 301004) using a PHOENIX M2V stellar model ($T_{\rm eff} = 3500$ K, $\log g = 4.5$) normalized to $K = 9.7$ mag. For the observing setup in the ETC, we specified the BRIGHTSKY subarray, FASTR1 readout mode, and 39 groups per integration. Since the total time on target varies for each of the 4 eclipse observations in the 2-checkpoint strategy, the number of integrations per exposure is shown in Table 2 for each observation.

Our observational setup yields no errors or warnings in the ETC or in APT. Observation 4 was placed on hold to decide on possible changes to the phase constraints after Observation 3.

Table 2: Comprehensive Observation Planning Parameters for TOI-771 b

(c) Eclipse Observation Schedule

Phase constraints and exposure parameters from Tinker Scheduling analysis

Obs	$\phi_{\min}$	$\phi_{\max}$	t_0 (HJD)	t_{total} (hr)	n_{ints}
1	0.9394514	0.9573664	2461111.272	4.76	496
2	0.9393259	0.9572410	2461111.273	4.77	497
3	0.9375775	0.9554926	2461111.268	4.97	517
4	0.9188099	0.9367250	2461111.321	7.06	735

Table 3: APT input parameters for TOI-771 b.

APT Input Parameters

Based on `juliet` circular orbital solution (APT 2025.1, JWST ETC 4.1, Pandeia 4.0)

(b) MIRI Instrument Configuration

Parameter	**Value**	**Unit**
Detector Subarray	BRIGHTSKY	—
Number of Groups	39	—
Detector Settling Time	0.75	hr
Pre-eclipse Baseline	1.5	hr
Post-eclipse Baseline	1.5	hr
Eclipse Duration	1.0	hr

(c) Target Astrometric Parameters

Parameter	**Value**	**Unit**
Right Ascension (J2016.0)	10:56:27.338	h:m:s
Declination (J2016.0)	-72:59:06.663	d:m:s
Parallax	39.447	mas
Proper Motion (RA)	39.300	mas yr^{-1}
Proper Motion (Dec)	-76.417	mas yr^{-1}

References

Espinoza, N., Kossakowski, D., & Brahm, R. 2019, Monthly Notices of the Royal Astronomical Society, 490, 2262, doi: 10.1093/mnras/stz2688

Gaia Collaboration, Prusti, T., de Bruijne, J. H. J., et al. 2016, AAP, 595, A1, doi: 10.1051/0004-6361/201629272

Gaia Collaboration, Vallenari, A., Brown, A. G. A., et al. 2023, AAP, 674, A1, doi: 10.1051/0004-6361/202243940

Lacedelli, G., Pallé, E., Davis, Y. T., et al. 2025, AAP, 698, A223, doi: 10.1051/0004-6361/202554161

Speagle, J. S. 2020, Monthly Notices of the Royal Astronomical Society, 493, 3132, doi: 10.1093/mnras/staa278